ELASTO-PLASTIC BEHAVIOR OF BRACED FRAMES UNDER CYCLIC HORIZONTAL LOADING

by M. Yamada[I], B. Tsuji[II] and S. Nakanishi[III]

SYNOPSIS

To investigate the behavior of steel braced frames, cyclic horizontal loading tests are carried out using rectangular steel unit rigid frames with various kinds of bracings. Constant and incremental horizontal sway amplitude tests are conducted under the constant vertical load of the column. Deformation analysis is carried out using the three points model [1] as the cross section of the members and the Bauschinger model [2] as the behavior of the material. Elasto-plastic behavior of the braced frames including the post-buckling behavior of the bracing is clarified by the analysis. Fatigue life is investigated using range count method. The fact that fatigue life of the braced frame is relatively shorter than that of the unbraced frame is observed.

1. INTRODUCTION

A bracing is one of the main aseismic elements of the steel structure. In the case of the ordinary designed braced frames, the bracings yield in tension or buckle in compression before the frames begin to yield. The cyclic tests under the constant and incremental horizontal sway amplitudes are conducted using rectangular steel unit rigid frames with various kinds of bracings. Elasto-plastic behaviors are compared with the analytical results considering the Bauschinger effect of the material. Fatigue life is investigated using range count method.

2. ANALYSIS

Deformation analysis of the braced frames such as shown in Fig.1 are carried out under the following assumptions:

(1) Sections of frames and bracings are simplified into the equivalent three points model[1] with the same cross sectional area, moment of inertia and fully plastic moment as the original ones such as shown in Fig.1.

(2) Cyclic stress-strain relationship of the material such as shown in Fig.2 is obtained from the Bauschinger model[2].

Considering the buckling mode, the bracings are treated as the centrally compressed or tensioned simply supported bars effective length of which is a half length of the member. Each member is divided into twenty to thirty line elements and load-deformation relationships of the frames and bracings are obtained by the numerical integration procedure. Boundary conditions between the frame and the bracing are shown in Fig.3. Neglecting the axial deformation of the column, relations between axial displacement of the bracing δc and δt and horizontal and vertical displacement δh and δv of the frame are as follows. $\delta c=\delta t=2/\sqrt{5}\delta h$, for the single or X-type bracing and $\delta t=(\delta h-\delta v)/\sqrt{2}$, $\delta c=(\delta h+\delta v)/\sqrt{2}$, for the K-type bracing. Load-deformation relationships are obtained by the summation of the restoring forces of the frame and the bracing. Numerical results obtained are shown with broken lines in Figs.5 and 7.

I Professor of Structural Engineering, Faculty of Engrg., Kobe University.

II Assist. Professor, Faculty of Engrg., Kobe University, Kobe, Japan.

III Structural Engineer, Hirata Structural Engineers, Co., Osaka, Japan.

3.TEST

Four types of the specimens tested are shown in Fig.1. Unit rectangular rigid frames are made of rolled wide flange profile with the welded joints. The bracings with a built-up wide flange section are jointed to the frame using gusset plates and flat bar bracings are welded directly to the frame. Material properties are also shown in Fig.1. Except for the P9HT-type, specimens are made of the mild steel. The bracing of P9HT-type one is made of high tensile steel. Monotonous and cyclic horizontal loading tests are carried out under the action of the constant vertical loads of the column($N=1/3N_y$). Under cyclic loadings, constant horizontal sway amplitude tests($\delta ha=\pm 10mm, 20mm$) and incremental sway amplitude tests are conducted. The loading system is shown in Fig.4. The test specimen is set in the loading frame through pin-roller supports. The vertical load of the column is applied diagonally by the oil jack with load cell. To avoid the lateral buckling, beams are supported by the roller bearings. Displacements are measured by dial gages and strains by wire strain gages. The load-displacement curves obtained are shown in Figs.6-9 with solid lines.

4.DISCUSSIONS

4.1. Load-Displacement Relationship

Fig.5 shows the cyclic axial force-displacement relations of the bracings under the constant deformation amplitude. The solid line and the broken line show the experimental and the analytical results, respectively. The circles in the broken line indicate the state of stress at the center of the member. Under the compressive force, the buckling load or the maximum load is lowered by the Bauschinger effect and the residual tensile elongation of the member. Under the tensile force, axial stiffness deteriorates due to the buckling deflection. A short bracing shows the spindle shape loop and a long bracing shows the hardening type one. This is due to the fact that the buckling deformation vanishes in the plastic range in the former case and in the elastic range in the latter case. The coincidence between analytical and experimental results are very well. The behavior of the braced frames varies with the types and slenderness ratios of the bracing. Fig.6 shows the lateral force-displacement relationship of each specimen under the monotonous loading. Fig.7 shows the relationships under the constant horizontal sway amplitude of $\delta ha=\pm 10mm(R=1/60)$ and $\pm 20mm(1/30)$. The solid line shows the experimental results and broken line the analytical ones. The circles in the broken line show the state of stress at the bracing for the HRB-type specimens and at the column for the HRW-type ones. In the case of the unit rigid frames(HRW), the maximum resistance increases at the first few cycles through the strain hardening effect, and the elastic limit is lowered by the Bauschinger effect. In the case of the specimens with single bracing, the maximum resistance in the first quadrant increases with the cycles due to the strain hardening effect and decreases in the reversed loading due to the accumulated tensile elongation of the bracing. P9HT-type specimen with the most slender bracing shows the hardening type loop at the reversed loading. In the case of HX-type specimen, the buckling deformation of the bracing occurs only at one span and relatively large buckling deformation of the bracing is observed. Maximum resistance decreases with the increase of the number of cycles. Fig.7(j) shows the vertical deflection at the center of the beam of the HK-type specimen. The vertical force is added from the bracing after the buckling of the compression bracing. By this deflection, the extension of the tensile bracing is smaller than the contraction of the compressive one. The pattern of yielding of this frame is somewhat different from that of the other specimen. Fig.8 shows the pattern of yielding obtained by the analysis. The coincidence between analytical and experimental results are very well as shown in these figures. Fig.9 shows the load-displacement relationship at the incremental sway amplitude tests.

4.2. Fracture Mode and Fatigue Life

The cyclic loadings are continued until the deterioration of the lateral force or the crack propagation are observed. Fracture modes are shown in Table 1. The cracks are observed mainly at the welded joints. The breaking off of the bracing occured at the X-type bracing. In the case of HK-type specimen, the lateral deformation grows large. Fatigue life of the steel structures under the constant harmonic cyclic loadings may be expressed by the formula $N \cdot \delta_p^{\alpha} = \delta_{pf}$, where N, the number of cycles to fracture, δ_p, the plastic displacement amplitude and α is the constant. In the case of steel unit rigid frames, $\alpha=0.5$ was obtained from the experiment [2]. Using this value, δ_{pf} is caluculated by the range count method, and is shown in Table 1. The braced frames have relatively smaller value than the unbraced frames, except for P12 and HZ-type specimens under $\delta ha=\pm 20mm$, which are welded by the different method. The accumulated internal plastic energy ΣA_i is also indicated in the Table.

4.3. Equivalent Viscous Damping Coefficient Ratio

Fig.10 shows the relations between equivalent viscous damping coefficient ratio h_{eq} and the number of cycles. Because of the unsymmetrical nature of the single type bracing, the coefficient are obtained every half cycle. In the case of the constant amplitude tests, h_{eq} decreases gradually with the increase of the number of cycles, and increases with the increase of the horizontal sway amplitude. In the case of the incremental deformation amplitude tests, h_{eq} increases with the increase of the number of cycles.

5.CONCLUSIONS

Constant and incremental horizontal sway amplitude tests are carried out using rectangular steel unit rigid frames having various kinds of bracings such as shown in Fig.1. Elasto-plastic cyclic behavior of the braced frames including the post-buckling behavior of the bracing are clarified by the analysis using the three points model and the Bauschinger model(Figs.5 and 7). Fatigue life of the braced frames are discussed using range count method and it is observed that the life of the braced frames are shorter than that of the unbraced frame(Table 1).

6.BIBLIOGRAPHY

[1] Yamada,M., Sirakawa,K. : Elasto-plastische Biegeformanderungen von Stahlstützen mit I-Querschnitt, Teil II : Wechselseitig wiederholte Biegung unter konstanter Normalkrafteinwirkung, Der Stahlbau, 40. Jahrg., H.3, 1971 S.65-74 u. H.5, 1971 S.143-151.

[2] Yamada,M., Tsuji,B., and Murazumi,Y. : Elasto-plastic Cyclic Horizontal Sway Behavior of Wide Flange Unit Rigid Frames Subjected to Constant Vertical Loads, IABSE symp., Lisboa, Sep., 1973, pp.151-156.

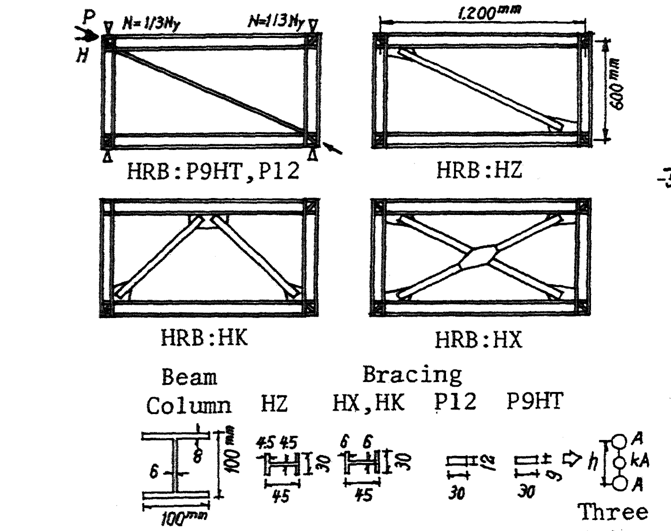

	Beam Column	Bracing HZ	Bracing HX,HK	Bracing P12	Bracing P9HT
h (mm)	90.9	20.0	19.2	8.0	6.0
k	0.37	2.26	1.40	0.67	0.67
$\sigma y(t/cm^2)$	2.88	2.77	2.75	2.64	5.50

Fig.1 Specimen

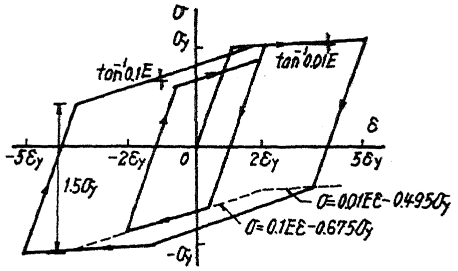

Fig.2 σ-ε Relation

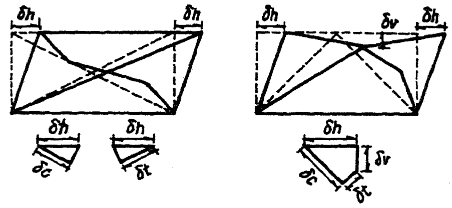

Fig.3 Boundary Conditions

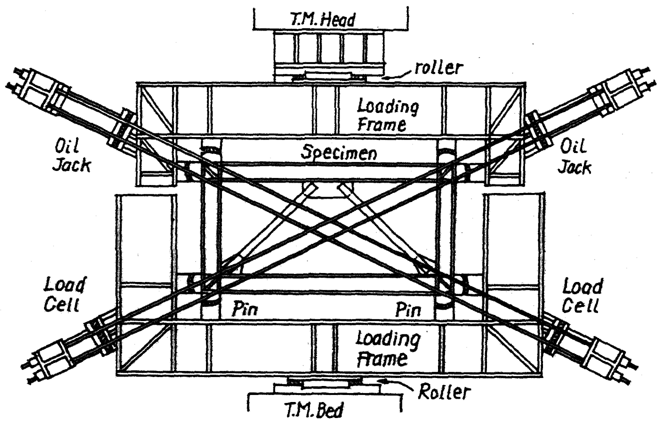

Fig.4 Loading System

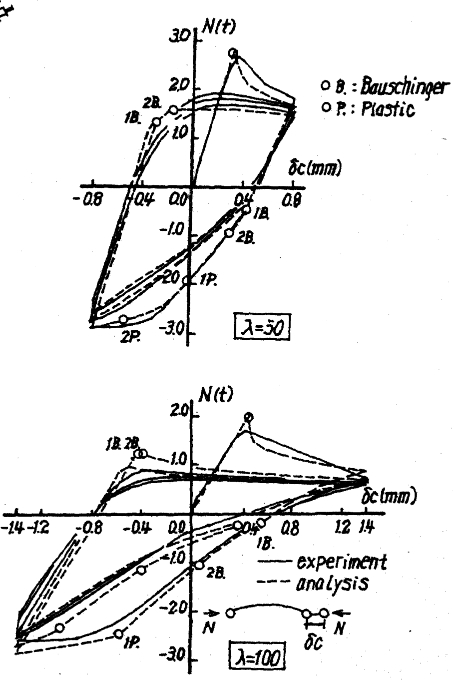

Fig.5 Axial Force-Displacement Relationship

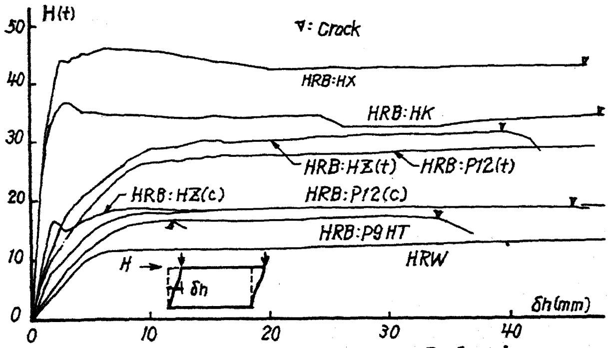

Fig.6 Load-Displacement Relations

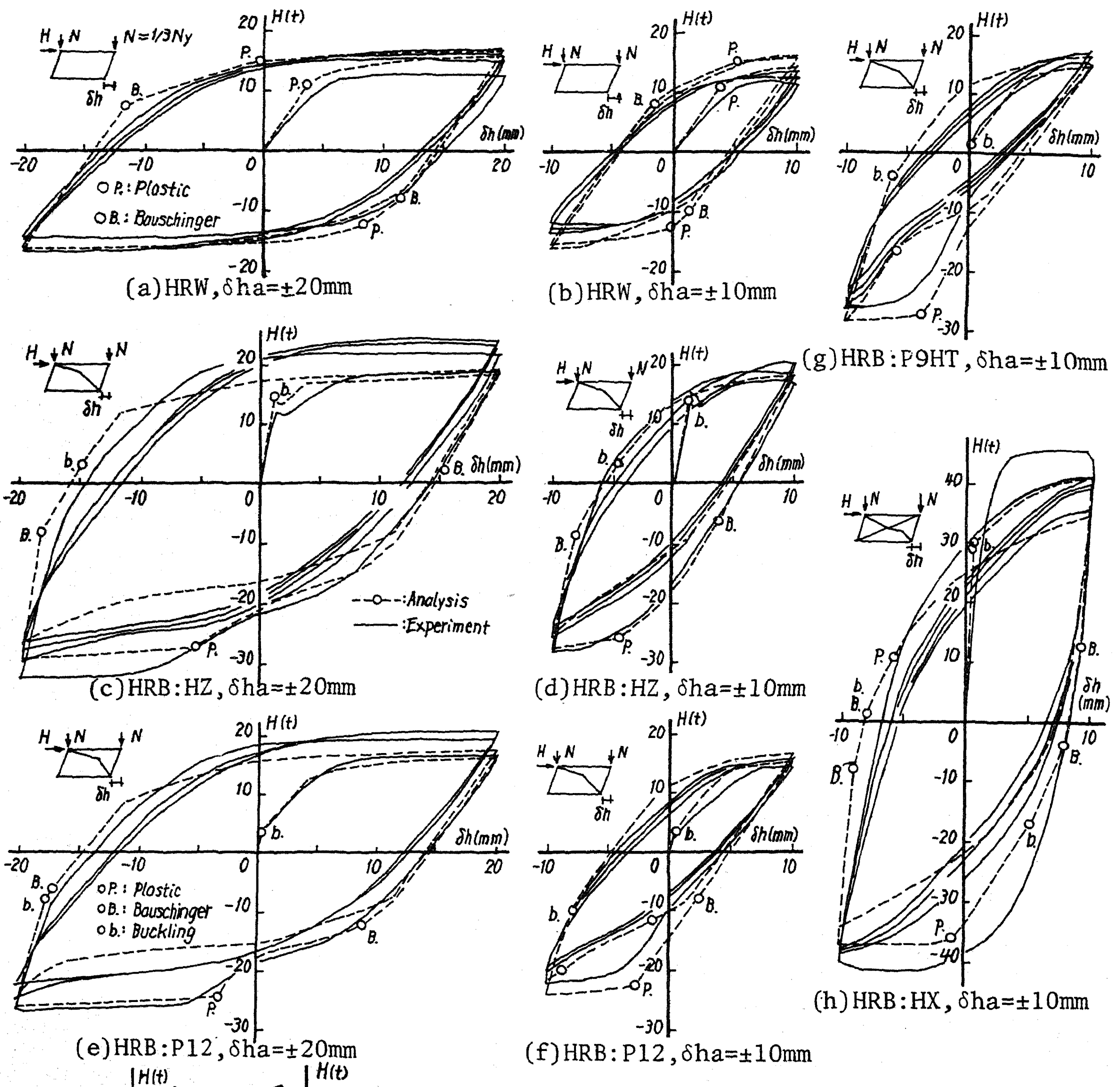

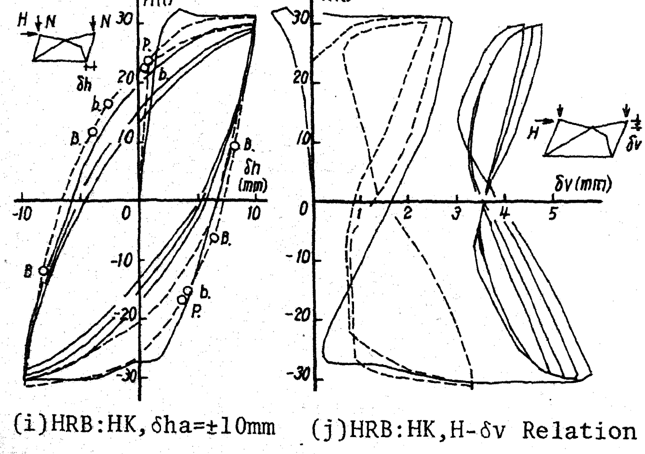

Fig.7 Load-Displacement Relationships

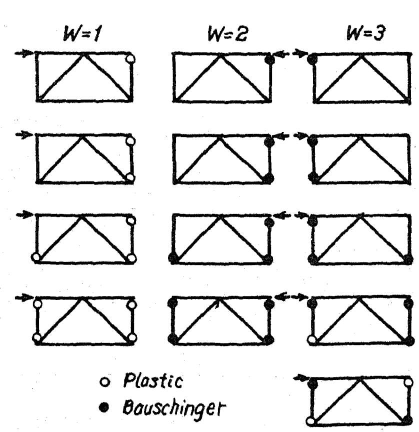

Fig.8 Yield Pattern (HRB:HK)

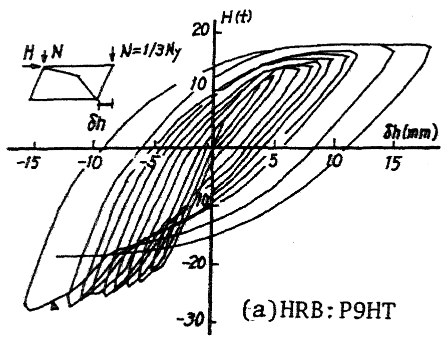

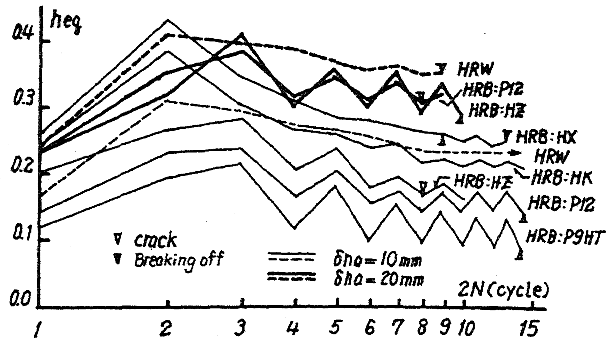

(a) Constant Amplitude Tests

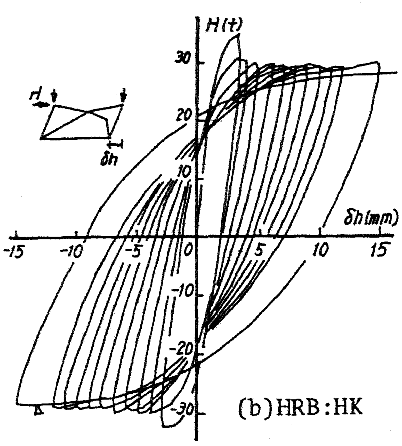

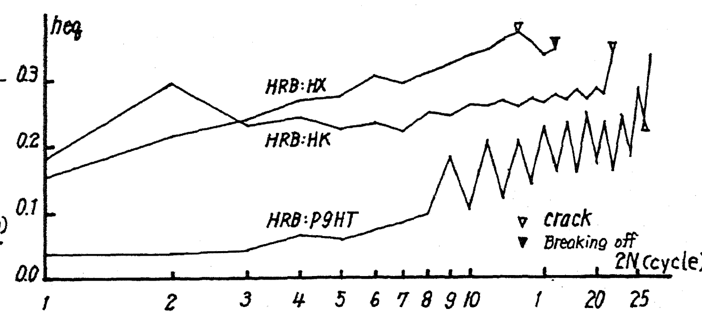

(b) Incremental Amplitude Tests

Fig.10 Equivalent Viscous Damping Coefficient Ratio

Table 1 Fatigue Life and Fracture Mode

	Monotonous Loading	Cyclic Loading		
		δha=+10mm	δha=+20mm	Increment.
	δpf(mm)	δpf(mm)	δpf(mm)	δpf(mm)
HRW	60 >	63.7 (A)	53.4 (A)	
HRB:P9HT	37.1 (A)	14.8 (A)		24.6 (A)
HRB:P12	60 >	18.1 (A)	59.7 (A)	
HRB:HZ	42.5 (C)	19.2 (B)	52.9 (B)	
HRB:HX	46.7 (B)	30.5 (B,C)		24.2 (B,C)
HRB:HK	48.1 (B)	31.1 (B.D)		31.6 (B,D)
		ΣAi (t·cm)	ΣAi (t·cm)	ΣAi (t·cm)
HRW		1046	326	
HRB:P9HT		120		230
HRB:P12		135	569	
HRB:HZ		146	514	
HRB:HX		470		451
HRB:HK		417		445

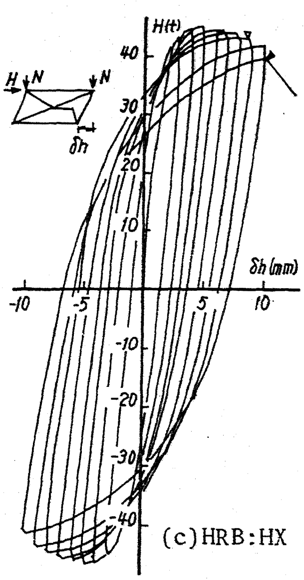

Fig.9 Load-Deflection Relations

(A) Crack at the Welding of Beam Column Joint
(B) Crack at the Welding of Gusset Plate
(C) Breaking off of Bracing
(D) Lateral Buckling of Whole Frame

DISCUSSION

N. Yoshida (Japan)

Sufficient of infinite ductility of the section is assumed in all analyses of brace. According to the result of experiment, however, several types of breakage of brace are observed, hence it seems that some kind of section don't have sufficient ductility. For the bracing members with wide flange or angle section, for example, local buckling takes place after flexural buckling, and large alternating plastic deformation concentrates at several sections due to local buckling. Hence braces are broken by the development of cracking due to low cycle fatigue at these sections. For steel pipe brace with gusset plate, cracking takes place at the front fillet welding at end connection in the early stage of loading, and breakage is propogated at this section.

Experimental result for various length and sections shows that low cycle failure (breakage) is important in braces with small slenderness ratio. In case of open section, width thickness ratio should be taken into consideration in addition to slenderness ratio.

Ajitha Simha (India)

Has the author (or any other) tried to test structures with definite shape, e.g. span/height ratio of 2. This ratio has been proved to be good for optimum design of structures - rigid frame portals in particular, with fixed bases, (work done in University of LIEGE, GELGIUM).

Author's Closure